

DESIGN AND INSTRUMENTATION OF A MULTI-MODAL  
IMAGING SYSTEM FOR BREAST CANCER DETECTION

Submitted To:

The Engineering Honors Committee

119 Hitchcock Hall

College of Engineering

The Ohio State University

Columbus, Ohio 43210

By:

*Joseph Ewing*

*1070 B Weybridge Rd. South.*

*Columbus, OH 43220*

*Date*

*November 13th, 2008*

## ACKNOWLEDGEMENTS

I would like to thank Dr. Ron Xu for all of his contributions, help and guidance in this research. I would also like to thank Hamid El-Dahdah, Bei Wang, Jiewei Huang and Jeff Xu for their assistance in testing and other procedures. Without the dedication and assistance of my lab group this research would not have been possible.

I would also like to acknowledge equipment support from Drs. Jay Zweier at David Heart and Lung Research Institute and Dr. Mark Walter at Department of Mechanical Engineering of The Ohio State University.

Funding support was provided by the Wallace Coulter Foundation Early Career Translational Research Award.

## ABSTRACT

Breast cancer is the leading newly diagnosed cancer among women in the United States and the second leading cause of cancer deaths. This makes accurate and early diagnosis a priority. However there is controversy and problems with current diagnostic techniques such as a lack of functional measurements from Mammograms and MRI's. Due to these limitations new techniques that overcome these problems such as combined Near Infra-red Ultrasound systems are desired. In this research an integrated dynamic Near Infra-red Ultrasound probe was developed to validate the ability of the system to produce accurate co-registered results. A second generation device was developed to use in a clinical trial that overcame the limitations of the benchtop probe. The benchtop probe produced accurate absorption properties of an embedded tissue simulating phantom. It was also proved that a user could be trained to follow within an accuracy of plus or minus 5% a computer generated pressure profile. These validation tests allowed for the system properties to be optimized prior to the current clinical trial. Future work will include implementing a contrast agent that is sensitive to both Near-Infra red and Ultrasound for better functional and structural measurements. The system could also be integrated with current cancer technology such as RF ablation to measure margins pre-operatively, intra-operatively, and post-operatively.

## TABLE OF CONTENTS

|  |       |
|--|-------|
| Acknowledgements.....                      | ii    |
| Abstract.....                              | iii   |
| Table of Contents.....                     | iv    |
| List of Figures.....                       | V     |
| Motivation and background.....             | 1-3   |
| Previous work.....                         | 3-4   |
| Theory.....                                | 4     |
| First Design Iteration.....                | 4-6   |
| Second Design Iteration.....               | 7-15  |
| NIR Function.....                          | 9-11  |
| Pressure Sensor Function.....              | 12-14 |
| Ultrasound Function.....                   | 14-15 |
| Methodology.....                           | 15-19 |
| Benchtop Testing.....                      | 15-16 |
| Compression Profile.....                   | 16-17 |
| Clinical Trial.....                        | 17-19 |
| Benchtop Results and discussion.....       | 19-22 |
| Clinical Trial Results and discussion..... | 22    |
| Conclusions.....                           | 22    |
| Future Work.....                           | 23-25 |
| References.....                            | 26    |

## LIST OF FIGURES AND TABLES

|  |    |
|--|----|
| Figure 1, Isometric view of first generation DNIRUS probe.....   | 5  |
| Figure 1, Detailed view of optical scanning mechanism of first<br>generation DNIRUS probe.....               | 5  |
| Figure 2, Bottom view details of first design iteration  |    |
| Figure 3, Isometric View of Second Generation DNIRUS Probe.....  | 6  |
| Figure 4, NIR Transmission Evolution, improvements in<br>Transmission.....                                   | 8  |
| Figure 5, Fiber Block Positioning.....   | 9  |
| Figure 6, Source and detector location.....  | 10 |
| Figure 7, Set Screw locations for Fiber Optics and<br>Block Placement.....                                   | 10 |
| Figure 8, Pressure sensor location first generation (left) ;<br>second generation (right).....               | 11 |
| Figure 9, pressure cylinder for use in FSR measurements.....   | 12 |
| Figure 10, Sensitivity property of the FSR's.....  | 13 |
| Figure 11, Electrical circuit used for FSR's.....  | 14 |
| Figure 12, Ultrasound window location.....   | 15 |
| Figure 13, Benchtop testing setup for first generation probe.....  | 16 |
| Figure 14, Calibration of the pressure sensors using load frame.....   | 17 |
| Figure 15, Clinical trial set up at James Care Cancer Center.....  | 18 |
| Figure 16, US image of the embedded tubing in tissue simulating<br>phantom.....                              | 19 |
| Figure 17, Correlation between actual and reconstructed<br>absorption levels. $R^2 = .999$ .....             | 20 |
| Figure 18, Details of compression profile.....   | 21 |
| Figure 19, Microbubble construction.....   | 24 |
| Figure 20, Micro and nano bubble distribution.....   | 24 |
| Figure 21, Possible use with cancer ablation detailed view of<br>iterative process for cancer treatment..... | 24 |

## **1. 0) Motivation and Background**

### **1.1) Motivation**

Among women in the United States, breast cancer remains the leading cause of newly diagnosed cases of cancer and the second leading cause of cancer deaths [1]. Detecting breast cancer at an early stage is associated with improved survival. However, there is controversy and debate regarding the effectiveness of the existing methods for breast cancer screening and early detection. First, statistics show that only about 20% of suspicious mammogram lesions in Breast Imaging Reporting and Data System (BIRADS) scale 3 to 5 are proven to be malignant on breast biopsy [2]. Second, little is known about the effectiveness of the clinical breast examination (CBE) due to the lack of performance consistency and standardization [3]. Third, breast self-examination (BSE) has not been shown to reduce breast cancer mortality [4]. In light of these limitations, the development and refinement of more innovative tools for analyzing the structural and physiologic characteristic of breast tissue for more precisely characterizing and differentiating malignant tumors, benign tumors, and normal breast tissue becomes increasingly important.

### **1.2) Background**

The mostly commonly used modalities for breast imaging are mammogram, ultrasound (US), and magnetic resonance imaging (MRI) [3]. These modalities primarily delineate the morphologic and structural characteristics of breast tissue. However, functional and physiologic properties of the breast can be characterized by such tools as positron emission tomography (PET) [6] and dynamic contrast-enhanced MRI (DCE-MRI) [7]. But the use of these methodologies for the breast are not yet considered

practical since they are viewed as experimental and are highly cost prohibitive. This is primarily due to the radioactive properties of PET and the high expense of a DCE-MRI exam as well as the fact that neither method is universally available. In this regard, it remains a priority to develop low cost, portable, noninvasive innovative imaging tools for better functional and structural characterization of the breast.

Near infrared (NIR) diffuse optical imaging and spectroscopy is capable of measuring multiple physiologic parameters of biological tissue systems and may have clinical applications for assessing the development and progression of neoplastic processes, including breast cancer and thus is an emerging modality for breast cancer detection in its early stages [5, 6]. NIR light in the range of 700nm-900nm can penetrate up to several centimeters into the tissue allowing for imaging of deeper tissue. However, the currently available application of near infrared imaging technology for the breast is compromised by low spatial resolution due to the exponential attenuation of light in biological tissue as well as multiple scattering properties. Also, tissue surface condition and the presence of measurement artifacts also make measurement accuracy and reproducibility questionable. In addition, tissue heterogeneities, inter-patient variations and cyclic hormone changes all contribute to a lack of universal diagnostic standards. In this regard, tumor geometric features obtained by other imaging modalities such as US can be used to guide the NIR image reconstruction [7, 8]. To overcome these limitations several techniques are being developed such as dynamic NIR imaging as well as combining NIR imaging with another modality such as US, MRI or mammograms to create a hybrid imaging system. Dynamic NIR imaging measures relative changes in tissue properties such as vasculature and hypoxia changes which leads to a relative

measurement of oxygen and hemoglobin. With these relative measurements, inter/intra patient variation error is minimized and a generalized diagnostic standard can be created. [12,13] Previous research has shown a correlation between high hemoglobin levels and low oxygen levels with a tissue lesion being malignant [9]. There are also changes that occur in tissue when a compressive force is applied, changing the oxygen and hemoglobin levels by as much as 12% [10].

### **1.3) Previous Work**

Previous work included the construction of a NIR imager for non invasive, *in-vivo*, dynamic detection of biological tissue anomalies [11]. This device was validated in a 50 patient clinical trial that included applied compressive forces and continuous measurements of hemodynamic responses. This trial indicated that suspicious breast lesions have lower [StO<sub>2</sub>] and higher [HbT] than the surrounding normal breast tissue [11,14-17]. The results of this trial indicate that pressure-induced [HbT] changes may have a correlation with malignant tumor characteristics [11]. The hypothesis that was developed as a result of this trial was that changes in the neovasculature process within tissue bearing cancer may cause an increase in vasculature resistance which causes a slower [Hbt] response than normal healthy tissue. This hypothesis was also verified with animal testing [11]. This clinical trial also resulted in a malignancy index being defined in an attempt to create a quantitative value from which patients can be diagnosed for malignancy conditions.

Limitations and complications within this system provide a need for the development of the Dynamic Near-Infrared Ultrasound (DNIRUS) probe. These include the fact the system used in this clinical trial had a relatively slow sampling rate which



was prohibitive for real time measurements. Also, the NIR device utilized a continuous wave function which means that tissue scattering properties were not able to be measured. In addition, the Ultrasound and NIR measurements were taken separately under different loading conditions and thus were not co-registered. The new DNIRUS probe will overcome these limitations.

## **2.0) Theory**

The general theory behind the DNIRUS probe is to combine multiple imaging modalities to utilize the positive aspects of each system and minimize the inconsistencies and problems with each system. This means obtaining physiologic tissue properties from deep tissue penetration from the NIR combined with the structural capabilities of US to perform image reconstruction. Dynamic pressure stimuli will also be induced on the breast tissue in order to minimize the variations between patients and within a single patient by measuring relative changes in tissue properties.

## **3.0) Materials and Apparatus**

### **3.1) First Design Iteration**

The first design iteration of the DNIRUS probe was constructed to validate the ideas behind the probe through benchtop testing. An isometric view of the first generation probe can be seen in figure 1.

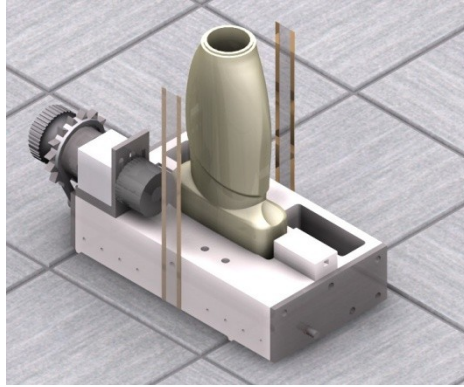


**Figure 22 Isometric view of DNIRUS probe**

The probe consists of a clinical ultrasound that snaps into the white delrin base with a custom made snap-in mechanism. There are two Force Sensing Resistors (FSR) from Tekscan Inc. that are attached to the bottom of the probe to measure the pressure changes induced during testing. An optical scanning mechanism is attached to the side of the probe that provides a method for manual movement of the NIR sources and detectors as well as a measurement knob. A detailed view of the optical scanning method is seen in Figure 2.

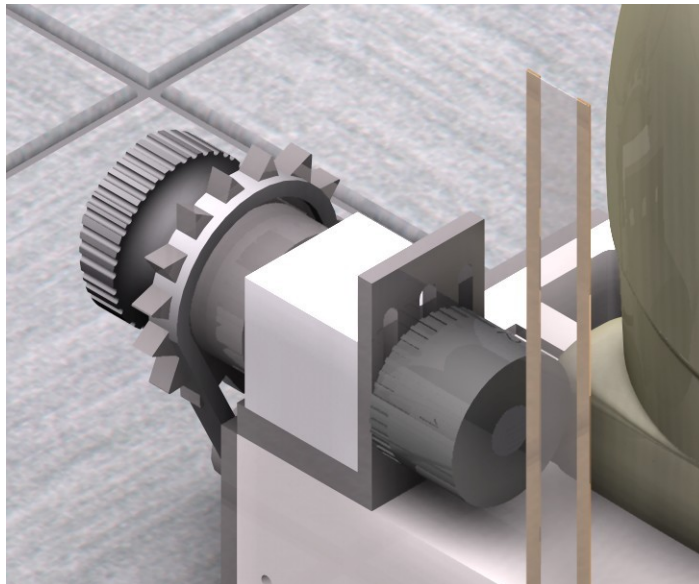


**Figure 23 Detailed view of Optical Scanning mechanism.**

The measurement knob with marks for length can be seen in Figure 2. The knob at the end of the device allows for manual movement. There is a timing belt that attaches the motion knob with the lead screws on the bottom of the probe that provide movement to the NIR sources and detectors. In figure three a bottom view of the probe can be seen.

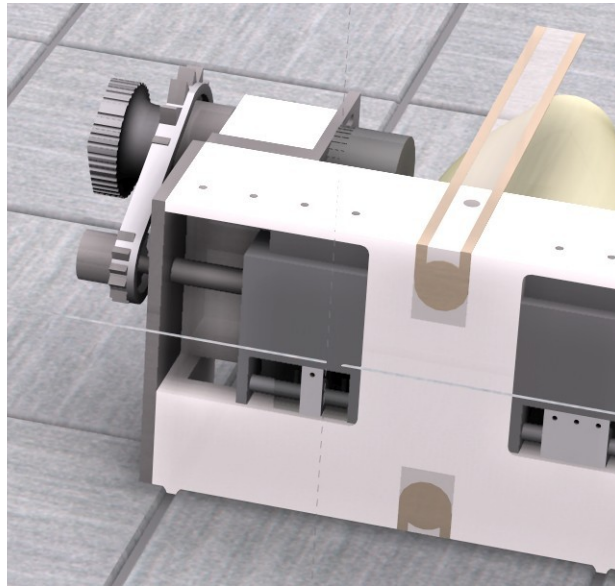


**Figure 24 Bottom view of first design iteration**

The timing belt attaches to lead screws on the bottom of the probe and provides opposite direction motion through one left handed lead screw and one right handed lead screw. The custom made fiber block holders can also be seen in Figure 3 attached to each of the lead screws. The NIR sources are mounted on one of the fiber blocks and the detectors are mounted on the other block. This design was used successfully to obtain verification data that the device had the potential to work as designed. However, due to certain limitations of the design, primarily that it was too bulky and complicated to be fully utilized in a clinical setting, a second design iteration was necessary.

### 3.2) Second Design Iteration

#### Materials List:

|  |                             |
|--|-----------------------------|
| Ultrasound Probe.....                                  | Terason model 128-10L5      |
| FSR Sensors.....                                       | Tekscan Inc. Model A-201    |
| ISS Tissue Oximeter with auxiliary module.....         | OxiplexTS™                  |
| Coupled Fiber Optic Cable (.5mm diameter).....         | Industrial Fiber Optics     |
| Fiber Optic Cable.....                                 | 2mm Industrial Fiber Optics |
| Custom Machined Parts<br>(OSU Chemistry Machine Shop): |                             |
| Prisms   |                             |
| Prism Holder   |                             |
| Base Block.  |                             |
| Pressure Cylinder                                      |                             |
| Handle   |                             |
| Cover  |                             |
| Machine Screws and Bolts (Various Sizes).....          | McMaster Carr               |
| 6v 300mA Power Supply.....                             | Radioshack                  |
| Capacitors.....  | Radioshack                  |
| Resistors.....   | Radioshack                  |
| Electrical Wire.....                                   | McMaster Carr               |
| Electrical Box.....                                    | McMaster Carr               |
| Belleville Washers.....                                | McMaster Carr               |
| Index Matching Gel.....                                | Industrial Fiber Optics     |
| Optical Epoxy.....                                     | Industrial Fiber Optics     |
| Polishing papers, varying grits.....                   | Industrial Fiber Optics     |
| Solid Ultrasound Gel.....                              | Fisher Labs                 |
| Liquid Ultrasound Gel.....                             | Fisher Labs                 |

The DNIRUS probe has been designed and constructed to meet certain criteria; principally that it is low cost, portable, and non-invasive. Other desirable characteristics that are lacking in current breast cancer detection methods that are desired for this DNIRUS system include improved reliability and combination of structural and physiologic modalities. The objective of the design was to successfully integrate into one functional unit NIR and US technology to measure tissue properties in response to dynamic stimuli. Other design requirements include being able to change the NIR source-detector separation, which was required to be able to take measurements at

varying tissue depths, the ability to accurately reproduce a computer generated pressure profile, clear high resolution US images, and high signal strength NIR readings. In addition, the DNIRUS probe will be used for clinical testing, and must be robust enough to withstand multiple tests and users.

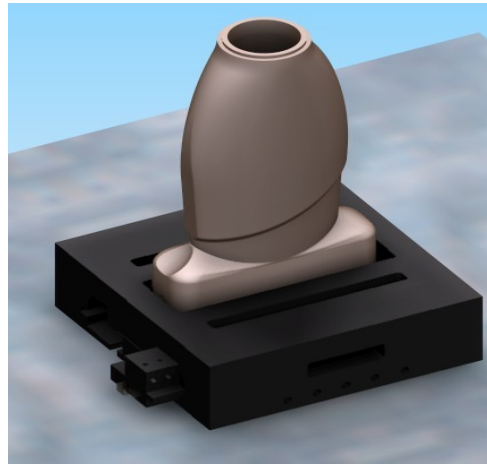


**Figure 25 Isometric View of Second Generation DNIRUS Probe**

A DNIRUS prototype includes adjustable blocks for NIR source-detector separation changes, pressure control (FlexiForce FSR sensors), near infrared sensor heads (connected to an OxiplexTS tissue oximeter), and a clinical ultrasound probe. The prototype is primarily operated in compression mode, where NIR diffuse reflectance measurements are collected at different angles around the suspicious lesion for baseline data and image reconstruction. Optical and physiologic properties of the breast lesion can be reconstructed with the spatial guidance provided by the ultrasound probe. During use, NIR diffuse reflectance and tumor deformation are continuously monitored as the DNIRUS probe is compressed against the suspicious breast tissue following a specific computer generated compression profile. Tissue optical and structural dynamics are calculated based on NIR and ultrasound measurements.

### 3.2 a) NIR Function

The NIR function begins at the OxiplexTS tissue oximeter, which provides the NIR source at both 690 nm and 830 nm wavelengths. The NIR is transmitted with a coupled .5mm fiber optic cable from the oximeter to the DNIRUS probe. This allows both wavelengths of light to be transmitted simultaneously along essentially the same fiber optic cable. Once the light is at the sensor head, it must accomplish a 90 degree bend. This manipulation is necessary to maneuver around the ultrasound sensor head, keeping the source-detector separation as close as possible, and make the NIR transmit from the bottom of the sensor head. This manipulation is accomplished by using a prism. This is represented by the dark brown shape in figure 5.

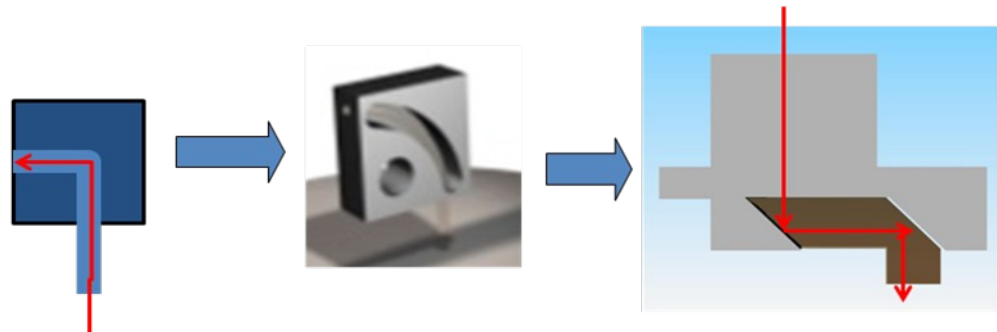


**Figure 26 NIR Transmission Evolution**

The evolution of the NIR transmission can be found in figure 5. The original design implemented a 90 degree bend directly into the fiber. This caused fiber damage and resulted in a light transmission of about 70% when compared to a straight fiber. This was recognized as a serious design flaw and the solution in the center of figure 5 was implemented. This utilized a bend radius to transmit the light. This increased the transmission to about 90% versus a straight fiber. Finally in the second generation design, a prism was utilized from which an efficiency of about 97% was realized.

The NIR is transmitted through the fiber optics to the top of the prism, and then reflects through the prism to exit out the bottom of the probe as shown in Figure 5 by the red arrows. The location of these blocks can be seen in figure 6 represented by the green block shapes. Index matching gel is applied at the contact areas between the prism and the fiber optic cable, as well as where the prism contacts the reflective material on the side of the block. This creates a more uniform contact surface and more efficient and predictable transmission pattern of light.

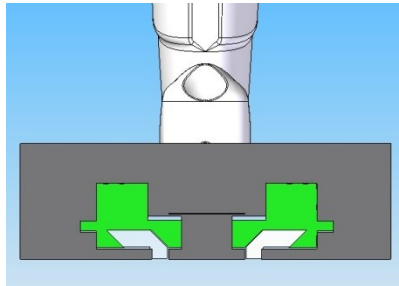


**Figure 27 Fiber Block Positioning**

The probe is designed to be able to use 8 sources as shown in figure 7, or one of the blocks can be removed to use only 4 sources. The eight sources are located on the right side of the block in figure 7 and the detectors are on the left.

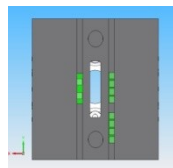


**Figure 28 Source and detector location**

For the clinical trial in the summer of 2008, 4 sources were used. The detector fibers used were single 2mm bare fibers. Because they were bare, a covering was applied after installation into the DNIRUS sensor head. This ensured that no ambient light was being picked up by the detector fibers, which minimized the error due to ambient light. The detectors also used the same 90 degree mechanism and holding block as the source fibers. Both fiber types were locked into place using a set screw as shown in figure 8. The holding blocks themselves are also able to be locked into place after they have manually been placed in the appropriate position by using set screws as shown in figure 8.

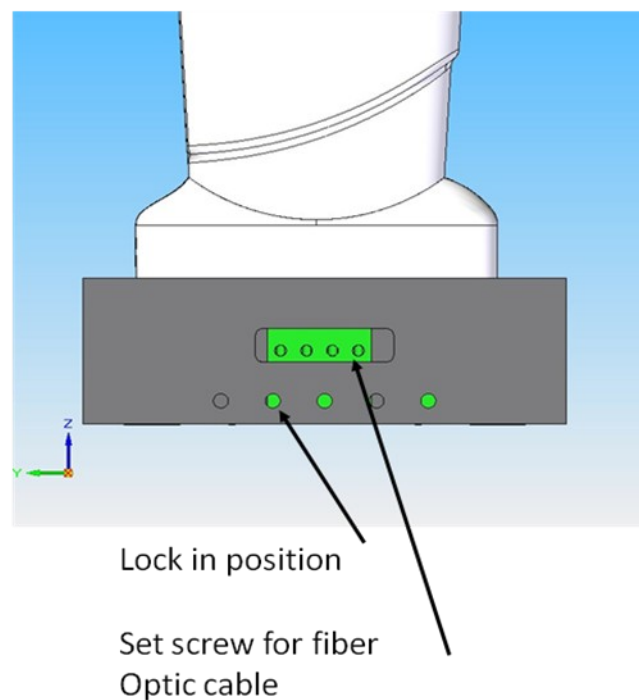


**Figure 29 Set Screw locations for Fiber Optics and Block Placement**

This allows for the fibers to be removed for maintenance and for the fiber block holders to be moved. This movement creates a change in the source detector separation and changes the depth of the NIR readings.



### 3.2 b) Pressure Sensor Function

The other main function of the DNIRUS probe is to monitor and record the pressure of the probe against the tissue. This is accomplished through Force Sensing Resistors (FSR) located on the bottom of the probe. The general location of these sensors can be seen in figure 9.

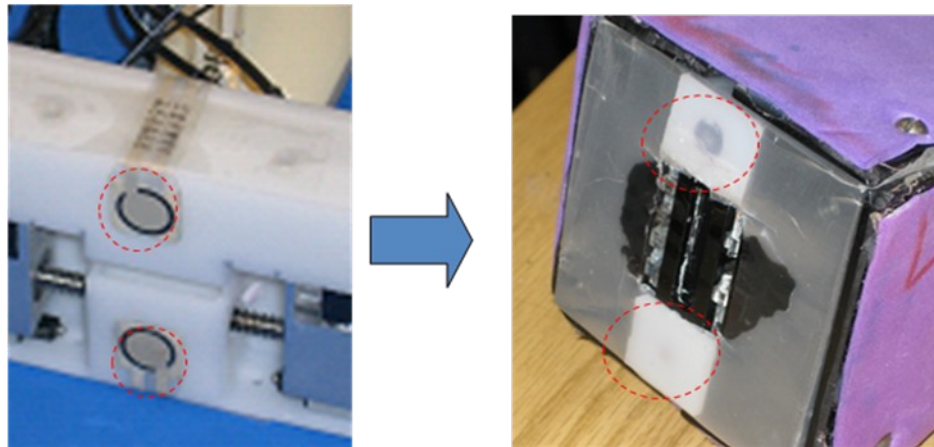


**Figure 30 Pressure Sensor Location First Generation (Left) ; Second Generation (Right)**

The mounting and incorporation of these sensors into the system changed from the first to second generation. The open mounting of the first generation was not appropriate for clinical testing, thus the sensors were imbedded into the probe through a slit in the side of the base. A “pressure cylinder” (figure 10) was added on top of the pressure sensors to measure the pressure at the surface.

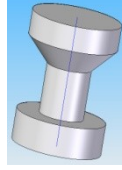


**Figure 31 Pressure Cylinder**

Belleville washers were also added between the pressure cylinder and the FSR's in order to provide a pre-load on the sensors. This was necessary due to the insensitive properties of the FSR's at low load levels. This is illustrated in figure 11.

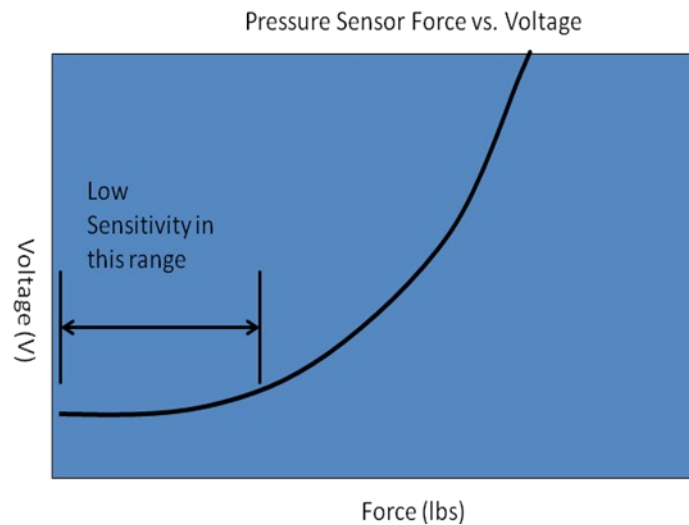


**Figure 32 Sensitivity property of the FSR's**

The pre-load was adjustable by a set screw that contacted the pressure cylinder in the sloped portion. As the set screw was tightened, it slid up the sloped portion of the cylinder, creating more pressure on the Belleville washer, more pre-load and therefore skipping past the insensitive range of the FSR's. In order to give stronger signal, the surface area of pressure sensors was increased by adding rectangular delrin pieces. These are white in figure 9. This increased the voltage output reading from about .25 volts to about 2.5 volts.

An amplifying circuit was also constructed to increase the sensitivity of the FSR's. The general circuit can be seen in figure 12. The resistor was added specifically to increase the sensitivity of the FSR's, meaning that a lower load would result in a higher voltage output. The capacitor was added to decrease the noise in the system and give a more consistent output.

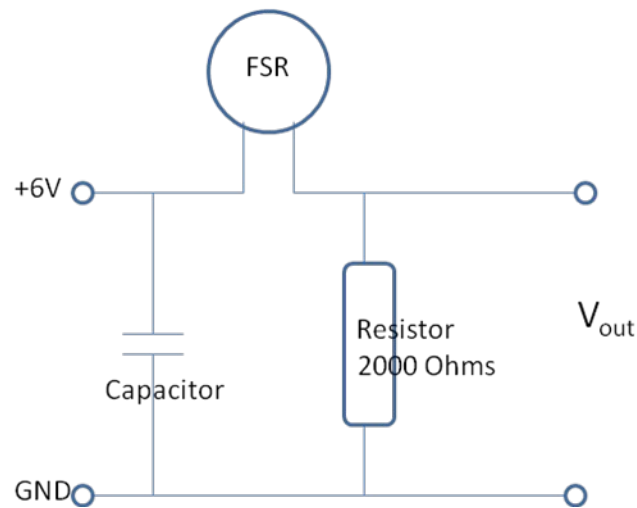


**Figure 33 Circuit used for FSR's**

One side of the probe contains the FSR previously described while the second side contains a pressure switch that outputs either an “on” signal of the input (about 6V) or an “off” signal of about 0V. This signal was necessary in ensure that if the FSR was not sufficiently sensitive on the breast tissue there is still some measure of pressure. This is not the anticipated case, but must be accounted for to ensure some measure of steady pressure exists. This sensor used the same circuit (figure 12) as the FSR, only the 2000 ohm resistor was replaced with a 200 ohm resistor.

### **3.2 c) Ultrasound Function**

The remaining modality of the probe is the Ultrasound. This consists of the clinical Ultrasound probe and an ultrasound transducer. The main design implementation for the Ultrasound was to design a snap in mechanism to fix the Ultrasound to the base. It also needed to have a clear path to obtain its signal without interference from the NIR while also measuring from the same location as the NIR readings were being taken thus ensuring a co-registration of the images. A spring loaded snap in device was constructed to meet these requirements. Also, a hole was cut through the base to the bottom of the Ultrasound probe to allow for a clear signal path. This hole location can be seen in figure 13 outlined in red.

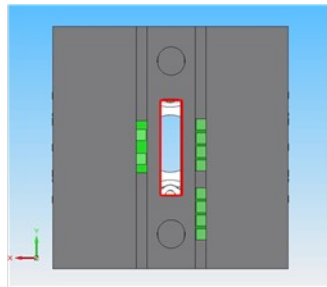


**Figure 34 Ultrasound window location**

#### **4.0) Methodology**

##### **4.1) Benchtop Testing**

Additional Materials List:

- Peristaltic Pump
- Tissue Simulating Phantom[18]
- Tubing (.40 cm diameter) ..... Fisher Labs
- India Ink..... McMaster Carr
- Dry Skim Milk..... Grocery
- Quiktest™ load frame microtester (Enduratec, Eden Prairie, MN)

The first generation probe was primarily constructed to verify the hypothesis of NIR and US co-registration to measure scattering and absorption properties in the blood. The general schematic for the bench-top test can be seen in figure 14.

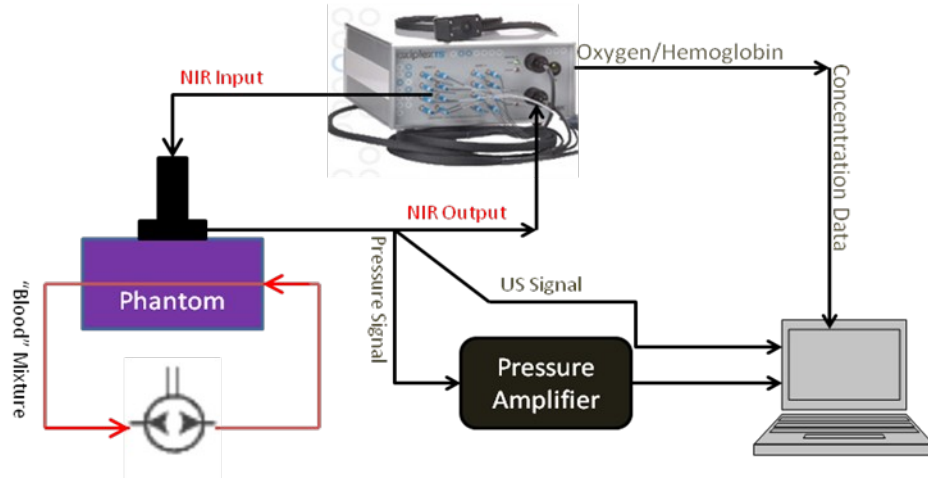


**Figure 35 Benchtop testing setup**

The testing procedure was to pump a mixture containing skim milk and India Ink through the tissue simulating phantom and record measurements with the probe. The tissue simulating phantom is a technology previously developed within our lab group [18]. The skim milk approximately matches the scattering properties of human tissue, and the India Ink was used to change the absorption properties. Ink was added in 25  $\mu\text{L}$  increments to the skim milk mixture to change the level of absorption. The concentration of skim milk could be adjusted to change the scattering coefficient of the mixture. At each new ink level, the absorption level was measured with both the Tissue Oximeter and with the DNIRUS probe. Ultrasound data was also simultaneously taken to produce a co-registered image reconstruction. The NIR and US data was then used to perform image reconstruction and calculate the simulated tumors absorption coefficients. This was then compared with the direct data taken from the Tissue Oximeter.

## 4.2) Compression Profile

In order to accurately measure the dynamic response of the tissue, an accurate pressure measurement had to be obtained. Since the probe is user controlled, not automated, this means that the user must be able to provide a constant steady pressure to the tissue. This feasibility was studied by generating a square wave profile using labview, then simultaneously plotting this profile with the real time pressure produced by the user. This gave a measure of how well a user could be trained to give a constant repeated pressure measurement.

The pressure sensors were calibrated using a Quiktest™ load frame microtester (Enduratec, Eden Prairie, MN). Loads from 0-5500 Pa were applied by the load frame on to the probe. Three measurements were taken at each load to minimize error. A fifth order polynomial was then fitted to the data points. This curve can be seen in figure 15.

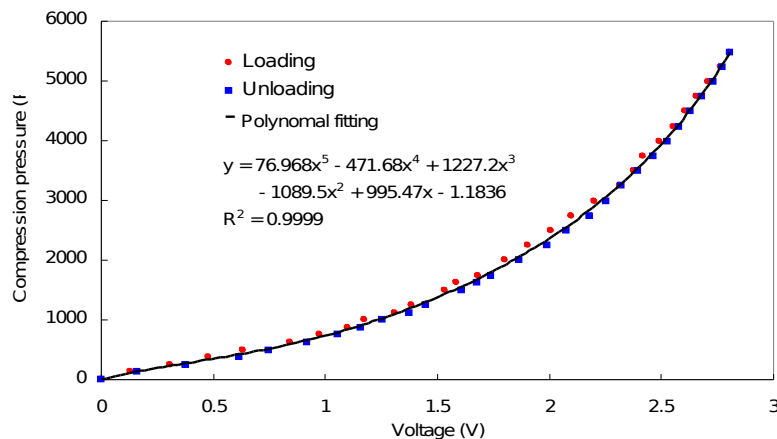


**Figure 36 Calibration of the pressure sensors**

The  $R^2$  value was greater than .9999, indicating a good fit of the curve to the data. Additionally, no significant hysteresis was observed during this testing. For the tests, a stepped compression profile was generated for the user to follow with a peak load of about 5000 Pa.

#### 4.3) Clinical Trial

The clinical trial is being conducted at the James Care Cancer Center in Dublin, Ohio. This clinical trial protocol has been approved by The Ohio State University Cancer IRB (protocol #: 2008C0006). The testing procedure begins after a patient has met the qualifications for the study and agreed to take part. The testing area and general setup can be seen in figure 16.

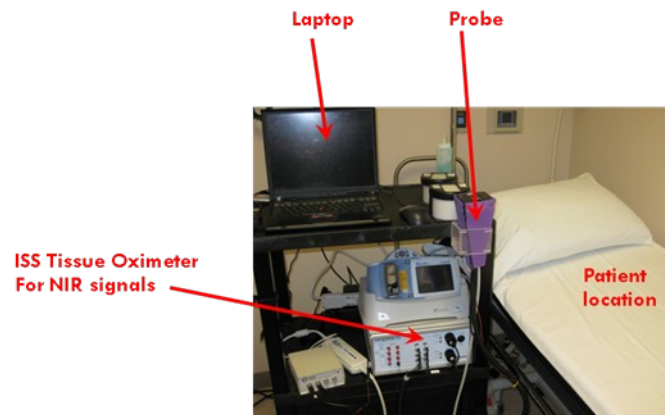


**Figure 37 Clinical trial set up**

A mammogram and Ultrasound are run according to normal testing procedures at the clinic. From this, a tumor location is found. The patient then moves to the testing room for the trial measurements while their mammogram and US tests are being analyzed.

Prior to the patient arriving, the system is calibrated with custom software developed by Hamid El-Dahdah from our lab group. This Labview software contains a Graphical User Interface for easy training. The trial testing begins with locating the tumor

with the US on the DNIRUS probe. After the tumor is located, preliminary images are taken at 0, 45, 90 and 135 degrees. These images are also taken at the identical location on the healthy breast. Next the stepped compression profile begins. The nurse follows the profile provided by the computer through 10 pressure peaks. This is repeated for a total of 5 tests. Then the same 5 tests are run on the healthy breast tissue for comparison background data to be used when the data analysis is performed.

## 5.0) Results and Discussion

### 5.1) Bench Top Results

Figure 17 shows an Ultrasound image acquired during the benchtop testing of the first generation DNIRUS probe. From this Ultrasound image dimensions and location information was taken using a least square fitting technique. From this information reconstruction of the

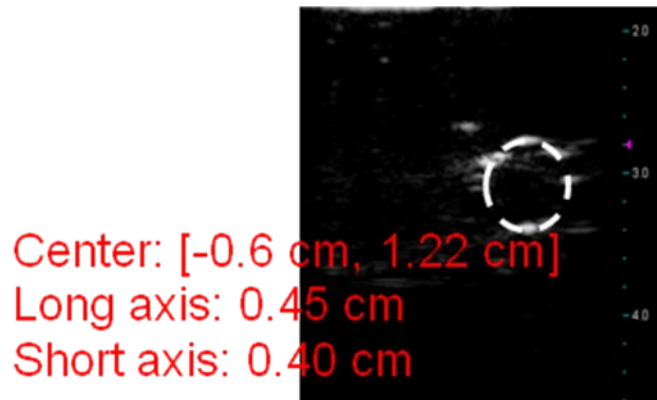


**Figure 38 US image of the embedded tubing in tissue simulating phantom**

embedded heterogeneity was performed and absorption information was determined. The absorption and scattering properties of the phantom were characterized by the Oxiplex™ tissue oximeter ( $\mu_a = 0.0147 \text{ cm}^{-1}$ ,  $\mu'_s = 5.2665 \text{ cm}^{-1}$ ). The data at the first ink concentration level was used as the calibration. Figure 18 shows a graph of the actual absorption levels versus the reconstructed levels. This data had an  $R^2$  value of greater



than .989. There are several possible sources of error from these tests which include a mismatched boundary condition at the gel wax-liquid interface, NIR measurement error in the background absorption and scattering coefficients, as well as error in the Ultrasound measurement of the tubing location and dimensions. These errors can be reduced by using an embedded solid tumor simulator and improving the US algorithms as well as obtaining more accurate NIR measurements.

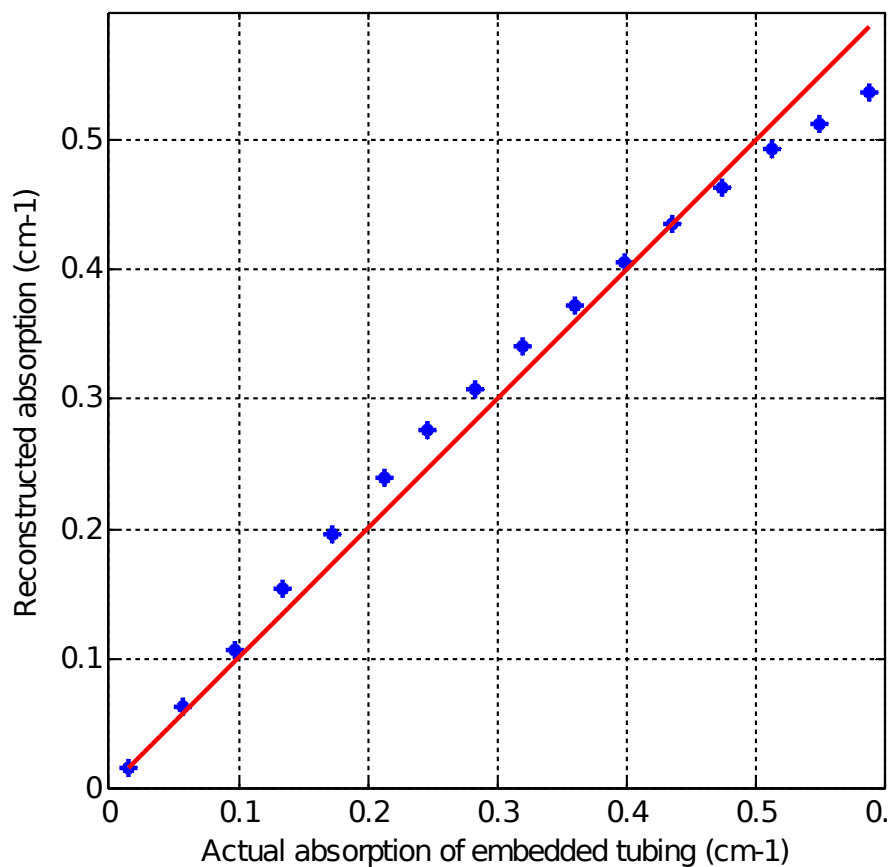


**Figure 39 Correlation between actual and reconstructed absorption levels.  $R^2 = .999$**

Other limitations of the system include that it can only solve for four unknown variables. Since breast tissue is almost always heterogeneous, it is necessary to include the ability to solve for more than one unknown heterogeneity. The system can

accomplish this as long as the boundaries are clearly defined. If the tissue has more than four unknown heterogeneities then the system may not be appropriate. This could be overcome by adding more optical measurements and improving the imaging algorithm. Another limitation of the system is that unlike the essentially two dimensional tubing used in the benchtop testing, a tumor is 3D. This is overcome by taking cross sectional Ultrasound measurements from different angles and then estimating the 3D geometry from these images. An additional complication is that the structural boundary found from the Ultrasound may not represent the functional boundary found from the NIR measurements. This could possibly be resolved in the short term by adding a computational offset to the Ultrasound measurements.

Figure 19 shows some detailed results of the compression testing. As previously noted, reliable pressure data is necessary in order to measure dynamic response of the breast tissue. In Figure 19, the dashed line represents the computer generated profile and the solid line is the user response to the profile. Data to note from this figure is that the average time delay during the

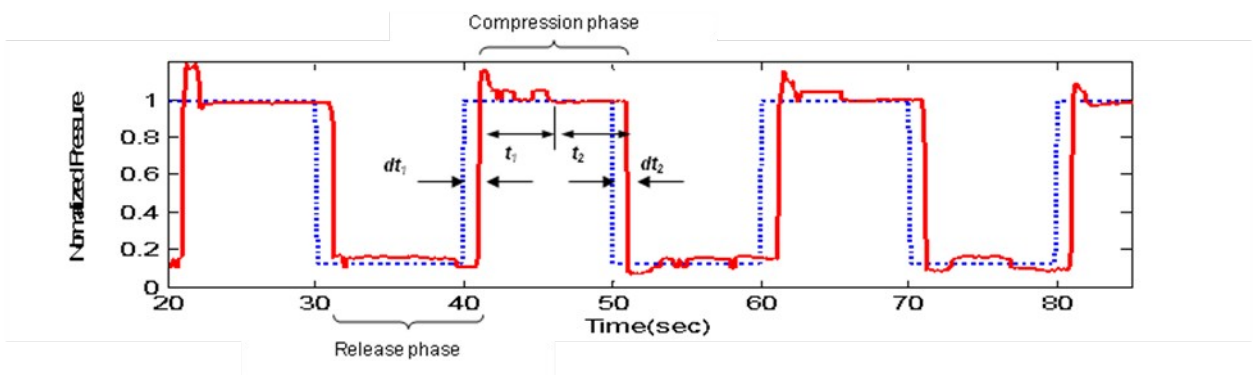


**Figure 40 Details of compression profile**

compression ( $dt_1$  in Figure 19) is  $0.905 \pm 0.035$  second; and the averaged release time delay  $dt_2$  is  $1.083 \pm 0.110$  second. You can also observe that there is some fluctuation during the first part of the compression phase,  $t_1$  which is followed by a much more stable phase,  $t_2$ . This stable compression phase was repeated in each of the five subjects who performed this test. The results of the tests were analyzed and it was found that during  $t_2$  the accuracy of the compression load reaches 95.7% of the compression target and the relative pressure deviation is less than 5%. It is within this time phase that the NIR measurements should be taken for maximum accuracy.

## **5.2) Clinical Trial Results**

The current clinical trial is still ongoing and does not have preliminary results yet. Testing for the clinical trial will continue until reliable data is taken with a clear boundary established by the Ultrasound. This data will then be analyzed to determine if the hypothesis that changes in the neovasculature process within tissue bearing cancer may cause an increase in vasculature resistance which causes a slower [Hbt] response than normal healthy tissue is true, as well as that high hemoglobin levels and low oxygen levels are associated with a tissue lesion being malignant.

## **6.0) Conclusions and Future Work**

### **6.1) Conclusions**

In conclusion a prototype was developed using the combined modalities of Near Infra red and Ultrasound to measure the relative changes of breast tissue in response to dynamic pressure stimuli. A benchtop model was constructed that validated the ability to accurately reconstruct the absorption properties of a tissue simulating phantom. The benchtop model also validated the ability of a user to accurately follow a computer

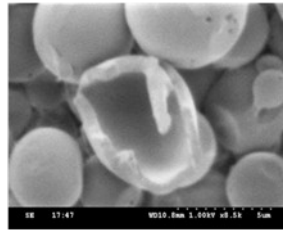
generated pressure profile. This data from benchtop testing is being used to optimize the clinical trial set-up. A second prototype was developed for use in the current ongoing clinical trial. The current clinical trial will be continued to obtain results to confirm the initial hypothesis.

## **6.2) Future Work**

There are many directions for the future work of this research to continue. Of primary importance is to finish the current clinical trial to validate the use of the combined modalities as a legitimate way to diagnose cancer malignancy. If the trial proves successful, modifications may be made to improve the malignancy index defined in previous clinical trials.

Some limitations of the current research include the inability of the orthogonal Ultrasound to obtain accurate images of the 3D breast lesions. The plan to overcome this liability is to integrate a 3D volumetric Ultrasound into the current system. Also, differences between the functional and structural boundaries could lead to inaccuracies of NIR measurements. This can be overcome through the use of a contrast agent that has both Ultrasound and NIR sensitivity. This would give an accurate co-registered NIR and US image. This could be accomplished with the help of micro and nano bubbles which could be injected with an encapsulated dual sensitive contrast agent. Some work is currently being done in our lab towards the construction of these bubbles. Figure 20 shows a SEM image of these bubbles constructed. Figure 21 shows the size distribution for the micro and nano bubbles. With an attached antibody that would create an attraction to the cancer site, the micro/nano bubbles would cluster at the cancer site. The

bubbles could then be broken through either the use of concentrated Ultrasound signals or some other method. The contrast agent inside would then be released, saturating the cancer site and creating an accurate functional and structural boundary.



SEM image

**Figure 41 Microbubble Construction**

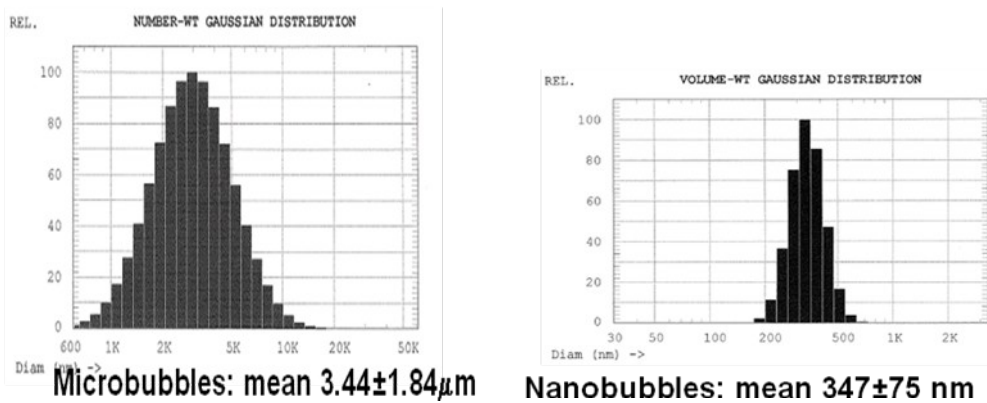
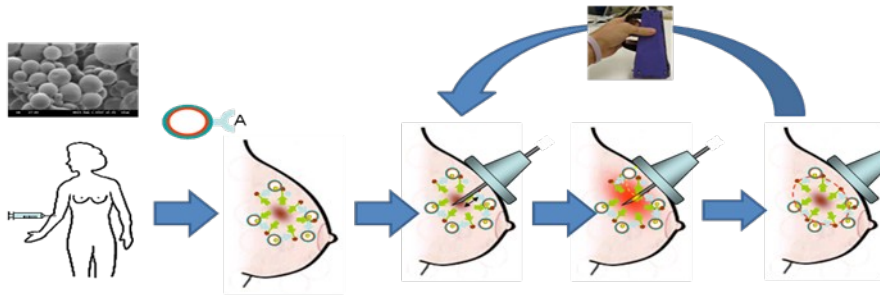


**Figure 42 Micro and nano bubble distribution**

This technology could then be integrated for use in other ways such as with cancer ablation. Figure 22 shows one way that this technology could be used to improve cancer treatment through ablation.



1:Microbubble → 2:Probe → 3:Ablation → 4:Monitor → Repeat 3,4

**Figure 43 Possible use with cancer ablation**

The basic process would be an injection of the contrast agent followed by pre-operative analysis using the DNIRUS technology to detect the tumor boundary. The system could then be used intra-operatively with cancer ablation techniques to monitor the boundary of tissue cooked. This would occur in an iterative process until it was determined the cancer was completely removed. Then a post operative analysis could be performed for a final check of the boundary. Utilization of this technology with current techniques such as Radio Frequency Ablation could lead to a significant decrease in breast cancer related deaths.

## REFERENCES

1. Jemal A, Siegel R, Ward E, Murray T, Xu J, Thun MJ: **Cancer statistics, 2007**. *CA Cancer J Clin* 2007, **57**:43-66.
2. Mendez A, Cabanillas F, Echenique M, Malekshamran K, Perez I, Ramos E: **Mammographic features and correlation with biopsy findings using 11-gauge stereotactic vacuum-assisted breast biopsy (SVABB)**. *Ann Oncol* 2004, **15**:450-454.
3. Mincey BA, Perez EA: **Advances in screening, diagnosis, and treatment of breast cancer**. *Mayo Clin Proc* 2004, **79**:810-816.
4. Thomas DB, Gao DL, Ray RM, Wang WW, Allison CJ, Chen FL, Porter P, Hu YW, Zhao GL, Pan LD, et al: **Randomized trial of breast self-examination in Shanghai: final results**. *J Natl Cancer Inst* 2002, **94**:1445-1457.
5. Xu RX, Qiang B, Mao JJ, Povoski SP: **Development of a handheld near infrared imager for dynamic characterization of in vivo biological tissue systems**. *Appl Opt*, in press.
6. Xu RX, Povoski SP: **Diffuse optical imaging and spectroscopy for cancer**. *Expert Rev Med Devices* 2007, **4**:83-95.
7. Xu RX, Povoski SP, Yee LD, Olsen JO, Qiang B, Mao JM: **Near Infrared/ Ultrasound Dual Modal Imaging for Breast Cancer Detection**. *Proc SPIE* 2006, **6081**:44-53.
8. Zhu Q, Huang M, Chen N, Zarfes K, Jagjivan B, Kane M, Hedge P, Kurtzman SH: **Ultrasound-guided optical tomographic imaging of malignant and benign breast lesions: initial clinical results of 19 cases**. *Neoplasia* 2003, **5**:379-388.
9. Chance B, Nioka S, Zhang J, Conant EF, Hwang E, Briest S, Orel SG, Schnall MD, Czerniecki BJ: **Breast cancer detection based on incremental biochemical and physiological properties of breast cancers: a six-year, two-site study**. *Acad Radiol* 2005, **12**:925-933.
10. Jiang S, Pogue BW, Paulsen KD, Kogel C, Poplack S: **In vivo near-infrared spectral detection of pressure-induced changes in breast tissue**. *Optics Letters* 2003, **28**:1212-1214.
11. Xu, R., H. El-Dhadah, J. Ewing, B. Wang, and S. Povoski, **Design and benchtop validation of a handheld integrated dynamic breast**

- imaging system for noninvasive characterization of suspicious breast lesions.** *Technology in Cancer Research and Treatment*, Submitted, 2008.
12. Cheng X, Mao JM, Xu X, Elmandjra M, Bush R, Christenson L, OKeefe B, Bry J: **Post-occlusive reactive hyperemia in patients with peripheral vascular disease.** *Clin Hemorheol Microcirc* 2004, **31**:11-21.
13. Xu RX, Young DC, Mao JJ, Povoski SP: **A prospective pilot clinical trial evaluating the utility of a dynamic near-infrared imaging device for characterizing suspicious breast lesions.** *Breast Cancer Res* 2007, **9**:R88.
14. Shangguan H, Prahl S, Jacques S, Casperson L, Gregory K: **Pressure effects on soft tissues monitored by changes in tissue optical properties.** *Proc SPIE* 1998, 3254:366-371.
15. Cheng X, Xu X: **Study of the pressure effect in near infrared spectroscopy.** *Proc SPIE* 2003, 4955:397-406.
16. Jiang S, Pogue BW, Paulsen KD, Kogel C, Poplack S: **In vivo near-infrared spectral detection of pressure-induced changes in breast tissue.** *Optics Letters* 2003, **28**:1212-1214.
17. Chan EK, Sorg B, Protsenko D, O'Neil M, Motamedi M, Welch AJ: **Effects of Compression on Soft Tissue Optical Properties.** *IEEE Journal of Selected Topics in Quantum Electronics* 1996, **2**:943-950.
18. [Bei Wang](#), [Stephen P. Povoski](#), [Xianhua Cao](#), [Duxin Sun](#), and [Ronald X. Xu](#). **Dynamic schema for near infrared detection of pressure-induced changes in solid tumors.** *Applied Optics*, Vol. 47, Issue 16, pp. 3053-3063